DALTON
FULL PAPER

Synthesis of rhenium–platinum complexes bearing carbaborane ligands and their unusual dynamic behavior †

Dianne D. Ellis, Paul A. Jelliss and F. Gordon A. Stone *

Department of Chemistry & Biochemistry, Baylor University, Waco, TX 76798-7348, USA

Received 14th March 2000, Accepted 25th April 2000
Published on the Web 6th June 2000

Treatment of Cs[3,3,3-(CO)$_3$-*closo*-3,1,2-ReC$_2$B$_9$H$_{11}$] **1** with [Pt(NCMe)$_2${Ph$_2$P(CH$_2$)$_2$PPh$_2$}][BF$_4$]$_2$ yielded [3,3,3-(CO)$_3$-3,8-(Pt{Ph$_2$P(CH$_2$)$_2$PPh$_2$})-8-(μ-H)-*closo*-3,1,2-ReC$_2$B$_9$H$_{10}$][BF$_4$] **2b** as the sole product. The cation of salt **2b** is a bimetallic species with a Re–Pt bond bridged by a *nido*-7,8-C$_2$B$_9$H$_{11}$ ligand pentahapto coordinated to the rhenium and with the β-B–H bond in the ligating CCB*B*B ring of the carbaborane cage forming a 3-centre 2-electron B–H⋯Pt bond. Deprotonation of **2b** with strong bases gives an isomeric mixture of the complexes [3,3,3-(CO)$_3$-3,*n*-(Pt{Ph$_2$P(CH$_2$)$_2$PPh$_2$})-*closo*-3,1,2-ReC$_2$B$_9$H$_{10}$] **3a** (*n* = 4), **3b** (*n* = 8). The isomers are readily separated and the proportion of **3a** to **3b** formed is solvent- as well as base-dependent. In THF solutions of **2b** afford a 1 : 3 : 1 equilibrium mixture of **2b**, **3a**, and **3b**. Refluxing THF solutions of **1** with [Pt(H)(THF)(PEt$_3$)$_2$][BF$_4$] for several days yields a separable mixture of the isomers [3,3,3-(CO)$_3$-3,*n*-{Pt(PEt$_3$)$_2$}-*closo*-3,1,2-ReC$_2$B$_9$H$_{10}$] **4a** (*n* = 4), **4b** (*n* = 8). The same reactants, when stirred together in CH$_2$Cl$_2$ at ambient temperatures, give **4a** and [3,3,3-(CO)$_3$-3,8-{Pt(H)(PEt$_3$)}-8-(μ-H)-*closo*-3,1,2-ReC$_2$B$_9$H$_{10}$] **5**. Complex **4a**, not **5**, is the precursor to **4b**, the interconversion occurring at elevated temperatures in solution by an intramolecular exchange of B–Pt σ bonds between α-B and β-B vertices in the coordinating CCBBB face of the cage. Treatment of **1** with [Pt(Me)(THF)-(PMe$_2$Ph)$_2$][BF$_4$] at room temperature initially gives [3,3,3-(CO)$_3$-3,4-{Pt(PMe$_2$Ph)$_2$}-*closo*-3,1,2-ReC$_2$B$_9$H$_{10}$] **6a**. However, **6a** isomerizes in CH$_2$Cl$_2$ solutions at ambient temperatures to give a 1 : 1 mixture of **6a** and [3,3,3-(CO)$_3$-3,8-{Pt(PMe$_2$Ph)$_2$}-*closo*-3,1,2-ReC$_2$B$_9$H$_{10}$] **6b**. The NMR data (^{1}H, ^{13}C, ^{11}B and ^{31}P) for the new complexes are discussed.

In recent years many bimetal compounds containing rhenium and platinum have been reported[1] including the first species incorporating carbaborane ligands.[2] In the metallacarbaborane complexes, prepared using [N(PPh$_3$)$_2$]$_2$[2,2,2-(CO)$_3$-*closo*-2,1-ReCB$_{10}$H$_{11}$] as the precursor, the Re–Pt bonds are bridged by *nido*-7-CB$_{10}$H$_{11}$ fragments. The cage system is pentahapto coordinated to the rhenium to give a *closo*-2,1-ReCB$_{10}$H$_{11}$ framework and a platinum–phosphine fragment is exopolyhedrally attached by a Re–Pt bond and an agostic B–H⋯Pt bridge. We have recently carried out studies with the more familiar *nido*-7,8-C$_2$B$_9$H$_{11}$ group, employing the complex salt Cs[3,3,3-(CO)$_3$-*closo*-3,1,2-ReC$_2$B$_9$H$_{11}$] **1**[3] in reactions with mid- to late-transition metal fragments, including iron, ruthenium, rhodium, copper and silver.[4] The Group 1B metal reagents gave species having Re–Cu and Re–Ag bonds in their solid state structures, while the remainder gave a novel class of *exo-closo* complexes with no direct Re–M bonds. We have now further developed this work, describing herein the syntheses from **1** of rhenium–platinum complexes and demonstrating the fragility of the Re–Pt bonds formed in some of the products. This lability leads to a remarkable intramolecular exchange of *exo*-B–Pt σ bonds between boron vertices in the coordinating face of the cage ligand.

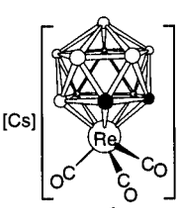

1

Results and discussion

The salt [Pt(NCMe)$_2${Ph$_2$P(CH$_2$)$_2$PPh$_2$}][BF$_4$]$_2$, formed *in situ* by treating [PtCl$_2${Ph$_2$P(CH$_2$)$_2$PPh$_2$}] with 2 mol equivalents of Ag[BF$_4$] in MeCN, was treated with salt **1**. Reaction occurred to afford in high yield a complex of composition [(CO)$_3$-{Pt(PEt$_3$)$_2$}-*closo*-ReC$_2$B$_9$H$_{10}$] **2**. As discussed below, detailed examination of the NMR spectra and a single crystal X-ray crystallographic study revealed that this product was [3,3,3-(CO)$_3$-3,8-(Pt{Ph$_2$P(CH$_2$)$_2$PPh$_2$})-8-(μ-H)-*closo*-3,1,2-ReC$_2$B$_9$-H$_{10}$][BF$_4$] **2b** and contained a bridging carbaborane ligand. There was no evidence for formation of an isomer [3,3,3-(CO)$_3$-3,4-(Pt{Ph$_2$P(CH$_2$)$_2$PPh$_2$})-4-(μ-H)-*closo*-3,1,2-ReC$_2$B$_9$H$_{10}$]-[BF$_4$] **2a**.

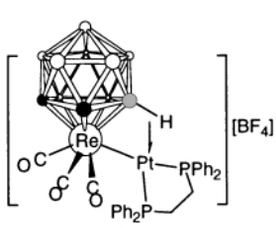

2a

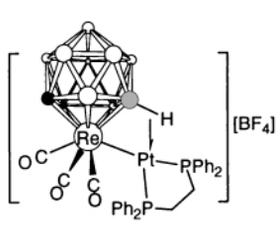

2b

† The compounds described in this paper have rhenium atoms incorporated into *closo*-1,2-dicarba-3-rhenadodecaborane structures and most have *exo*-PtL$_2$ groups. For complexes with 3,4-PtL$_2$ fragments, it should be noted that such species are racemic and the 3,7-PtL$_2$ notation is equally valid. The former is used in the formulae according to IUPAC convention.

Electronic supplementary information (ESI) available: fully coupled and selectively decoupled ^{1}H NMR spectra of complex **5**. See http://www.rsc.org/suppdata/dt/b0/b002043p/

DOI: 10.1039/b002043p

Table 1 Analytical and physical data

Compound[a]	Yield (%)	$\tilde{\nu}_{max}$(CO)[b] (cm^{-1})	Analysis (%)[c] C	H
2b [3,3,3-$(CO)_3$-3,8-(Pt{$Ph_2P(CH_2)_2PPh_2$})-8-(μ-H)-*closo*-3,1,2-$ReC_2B_9H_{10}$][BF_4]	86	2053vs, 1993s, 1968s	34.4 (35.1)	3.3 (3.3)
3a [3,3,3-$(CO)_3$-3,4-(Pt{$Ph_2P(CH_2)_2PPh_2$})-*closo*-3,1,2-$ReC_2B_9H_{10}$]	50	2022vs, 1952s, 1933s	36.9 (37.4)	3.5 (3.4)
3b [3,3,3-$(CO)_3$-3,8-(Pt{$Ph_2P(CH_2)_2PPh_2$})-*closo*-3,1,2-$ReC_2B_9H_{10}$]	25	2024vs, 1955s, 1929s	37.4 (37.4)	3.5 (3.4)
4a [3,3,3-$(CO)_3$-3,4-{$Pt(PEt_3)_2$}-*closo*-3,1,2-$ReC_2B_9H_{10}$]	21[d]	2020vs, 1949s, 1921s	24.8 (24.5)	4.8 (4.8)
4b [3,3,3-$(CO)_3$-3,8-{$Pt(PEt_3)_2$}-*closo*-3,1,2-$ReC_2B_9H_{10}$]	14	2018vs, 1945s, 1927s	24.5 (24.5)	4.8 (4.8)
5 [3,3,3-$(CO)_3$-3,8-{Pt(H)(PEt_3)}-8-(μ-H)-*closo*-3,1,2-$ReC_2B_9H_{10}$]	42	2034vs, 1962s, 1950s	18.7 (18.4)	3.8 (3.8)
6 [3,3,3-$(CO)_3$-3,*n*-{$Pt(PMe_2Ph)_2$}-*closo*-3,1,2-$ReC_2B_9H_{10}$] (*n* = 4 or 8)[e]	12	2021vs, 1950s, 1920s	28.0 (28.5)	3.6 (3.5)[f]

[a] All compounds are yellow. [b] Measured in CH_2Cl_2; medium-intensity broad bands observed at *ca.* 2550 cm^{-1} in the spectra of all the compounds are due to B–H absorptions. [c] Calculated values are given in parentheses. [d] Yield reported for preparation in CH_2Cl_2 at 25 °C. Yield when prepared in refluxing THF is 7%. [e] Compounds **6a** and **6b** cannot be isolated separately (see text). Therefore the overall yield, IR spectrum and microanalytical data for the 1 : 1 mixture are reported. [f] Contains 1.0 mol equivalent CH_2Cl_2, confirmed by NMR.

Table 2 Hydrogen-1 and carbon-13 NMR data[a]

Compound	^1H[b]	^{13}C[c]
2b	7.48–7.81 (m, 20 H, Ph), 3.63 [br s, 2 H, cage CH, *J*(PtH) = 38], 2.98 [ddt, 2 H, CH_2, *J*(PH) = 32, 7, *J*(HH) = 7], 2.61 [ddt, 2 H, CH_2, *J*(PH) = 29, 8, *J*(HH) = 8], −4.86 [br m, 1 H, B–H⟶Pt, *J*(PtH) ≈ 550]	190.0 (CO × 1), 186.6 [CO × 2, *J*(PtC) = 47], 134.6–124.9 (Ph), 38.1 (cage CH), 31.1 [dd, CH_2, *J*(PC) = 44, 8, *J*(PtC) = 74], 23.6 [dd, CH_2, *J*(PC) = 40, 6, *J*(PtC) = 59]
3a	7.72–7.37 (m, 20 H, Ph), 3.79, 3.36 (br s × 2, 2 H, cage CH), 2.35–2.11 (br m, 4 H, CH_2 × 2)	192.7, 192.6, 192.5 (CO × 3), 133.9–128.8 (Ph), 44.4, 36.2 (cage CH × 2), 31.3 [dd, CH_2, *J*(PC) = 19, 19], 26.9 [dd, CH_2, *J*(PC) = 9, 24]
3b	7.75–7.37 (m, 20 H, Ph), 3.37 (br s, 2 H, cage CH), 2.34–2.11 (br m, 4 H, CH_2 × 2)	192.1 (br, CO), 134.2–128.6 (Ph), 34.4 (cage CH), 31.0 [dd, CH_2, *J*(PC) = 20, 38], 27.1 [dd, CH_2, *J*(PC) = 8, 31]
4a[d]	3.87, 3.28 (br s × 2, 2 H, cage CH), 1.92 (br m, 12 H, CH_2), 1.01 [dt, 9 H, Me, *J*(PH) = 8, *J*(HH) = 7], 0.89 [dt, 9 H, Me, *J*(PH) = 11, *J*(HH) = 7]	196.9, 192.7, 191.7 (CO × 3), 44.5, 34.2 (cage CH × 2), 17.4 [d, CH_2, *J*(PC) = 32], 17.3 [d, CH_2, *J*(PC) = 20], 8.4, 8.2 (Me × 2)
4b[e]	3.31 (br s, 2 H, cage CH), 1.90, 1.72 (br m × 2, 12 H, CH_2), 0.98 [dt, 9 H, Me, *J*(PH) = 7, *J*(HH) = 6], 0.84 [dt, 9 H, Me, *J*(PH) = 9, *J*(HH) = 6]	197.2 (CO), 191.0 (CO × 2), 33.3 (cage CH), 17.6–17.1 (br m, CH_2 × 2), 8.3, 7.9 (Me × 2)
5	3.42 (br s, 2 H, cage CH), 1.97 [dq, 6 H, CH_2, *J*(PH) = 11, *J*(HH) = 7, *J*(PtH) = 50], 1.09 [dt, 9 H, Me, *J*(PH) = 19, *J*(HH) = 7], −4.84 [dq, 1 H, B–H⟶Pt, *J*(HH) = 15, *J*(BH) = 60, *J*(PtH) ≈ 465], −11.03 [br s, 1 H, PtH, *J*(PtH) = 1090]	194.2 (CO), 186.6 (CO × 2), 35.4 (cage CH), 22.5 [d, CH_2, *J*(PC) = 39, *J*(PtC) = 70], 9.3 [d, Me, *J*(PC) = 2, *J*(PtC) = 39]
6a[f]	7.43–6.95 (m, 20 H, Ph), 4.05, 3.36 (br s × 2, 2 H, cage CH), 1.74 [dd, 6 H, PMe, *J*(PH) = 8, 3], 1.65 [dd, 6 H, PMe, *J*(PH) = 12, 11]	197.5, 197.1, 193.4 (CO × 3), 131.5–128.5 (Ph), 45.9 [cage CH, *J*(PtC) = 45], 41.4 (cage CH), 18.7, 16.9 [d × 2, PMe, *J*(PC) = 39, 25]
6b[f]	7.43–7.21 (m, 20 H, Ph), 3.41 (br s, 2 H, cage CH), 1.77–1.55 (br m, 12 H, PMe)	192.2 (CO), 191.8 (CO × 2), 131.0–128.9 (Ph), 34.5 (cage CH), 17.8 [dd, PMe, *J*(PC) = 40, 4], 16.7 [d, PMe, *J*(PC) = 24]

[a] Chemical shifts (δ) in ppm, coupling constants (*J*) in Hz, measurements at room temperature in CD_2Cl_2, unless otherwise stated. Often ^{195}Pt satellites could not be observed due to poor compound solubility. They are noted where unambiguously assignable. [b] Resonances for terminal BH protons occur as broad unresolved signals in the range δ *ca.* −2 to 3. Resonances for cage CH and B–H⟶Pt protons are described as broad, corresponding to approximate $\nu_{1/2}$ values of 10 and 300 Hz, respectively. [c] Hydrogen-1 decoupled, chemical shifts are positive to high frequency of $SiMe_4$. [d] Measured at −73 °C. [e] Measured at −90 °C. [f] Measured at −80 °C.

Complex **2b** constitutes a rare example of a cationic metallacarbaborane without a charge-compensating group bound to the polyhedral carbaborane framework. Much earlier we reported the syntheses of the bimetallic cationic complexes [1,2-Me_2-3,3-$(CO)_2$-3-(L)-3,4-(μ-H)$_2$-3,4-{$Pt(PEt_3)_2$}-8-($CH_2C_6H_4$-Me-4)-*closo*-3,1,2-$WC_2B_9H_7$][BF_4] (L = CO, $CNBu^t$ or PMe_3) in which a carbaborane ligand spans a W–Pt bond by virtue of a B–H⟶Pt bridge.[5] Other groups have synthesized a handful of monometallic cationic metallacarbaboranes with and without charge-compensating groups bound to a carbaborane vertex.[6] The IR spectrum of **2b** (Table 1) displays ν_{max}(CO) bands at 2053, 1993 and 1968 cm^{-1}, indicative of adduct formation between the monoanion of **1** [ν_{max}(CO) 2005 and 1905 cm^{-1}][3,4] and the dicationic fragment [Pt{$Ph_2P(CH_2)_2PPh_2$}]$^{2+}$. The ^1H NMR spectrum (Table 2) revealed the presence of a 3-centre 2-electron B–H⟶Pt agostic bond by displaying a broad resonance at δ −4.86, the signal showing no resolvable ^{11}B–^1H coupling but clearly straddled by broad ^{195}Pt satellites [*J*(PtH) ≈ 550 Hz]. The presence of the Pt-chelating $Ph_2P(CH_2)_2PPh_2$ ligand is confirmed in this and the ^{13}C-{^1H} NMR spectrum with peaks for the phenyl groups as well as the CH_2CH_2 moiety. The molecule is bisected by a mirror plane of symmetry, reflected in the observation of one signal both in the ^1H NMR spectrum for the cage CH groups [δ 3.63, *J*(PtH) = 38 Hz] and also in the ^{13}C-{^1H} NMR spectrum (δ 38.1). The molecular C_s symmetry is supported by the 1 : 1 : 3 : 2 : 2 pattern seen in the ^{11}B-{^1H} NMR spectrum (Table 3). The peak at δ 22.2 is split in the ^{11}B NMR spectrum into a doublet with ^{195}Pt satellites [*J*(HB) = 52, *J*(PtB) = 140 Hz] as is typical for a B–H⟶Pt moiety.[5,7] The *cis*-positional rigidity of the $Ph_2P(CH_2)_2PPh_2$ ligand about the platinum is revealed in the ^{31}P-{^1H} NMR spectrum by the appearance of two signals (δ 62.3 and 55.9) with ^{195}Pt satellite couplings of similar magnitude to each other [*J*(PtP) = 2955 and 3393 Hz, respectively]. The broadness of the latter resonance implies that the phosphorus nucleus from which it derives lies *transoid* with respect to the boron atom of the B–H⟶Pt group. All the NMR data strongly support the structure depicted, where a β-B atom in the $\overline{CCBBB}$ face coordinating the rhenium is participating in the agostic B–H⟶Pt group. To confirm the structure of the cation, especially the presence of the Re–Pt bond, single crystals of **2b** were grown and an X-ray diffraction study was carried out. The

Table 3 Boron-11 and phosphorus-31 NMR data[a]

Compound	^{11}B[b]	^{31}P[c]
2b	22.2 [1 B, B–H⟶Pt, *J*(HB) = 52, *J*(PtB) = 140], −0.5 (1 B), −1.2 (1 B, BF_4), −7.7 (3 B), −13.1 (2 B), −15.5 (2 B)	62.3 [*J*(PtP) = 2955], 55.9 [br, *J*(PtP) = 3393]
3a	37.7 [1 B, B–Pt, *J*(PtB) ≈ 485], 0.5 (1 B), −0.9 (1 B), −3.2 (1 B), −7.2 (1 B), −16.5 (2 B), −19.2 (2 B)	64.8 [br, *J*(PtP) = 2060], 48.0 [d, *J*(PP) = 6, *J*(PtP) = 4709]
3b	49.6 [1 B, B–Pt, *J*(PtB) ≈ 440], −4.1 (1 B), −8.2 (2 B), −10.7 (2 B), −16.3 (2 B), −23.3 (1 B)	65.4 [br, *J*(PtP) = 2050], 49.0 [d, *J*(PP) = 17, *J*(PtP) = 5158]
4a	34.5 [d, 1 B, B–Pt, *J*(PB) = 76, *J*(PtB) ≈ 580], 1.1 (1 B), −1.3 (1 B), −2.9 (1 B), −6.9 (1 B), −16.3 (2 B), −19.8 (2 B)	[d] 22.6 [*J*(PtP) = 4652], 22.3 [br, *J*(PtP) = 2093]
4b	45.6 [1 B, B–Pt, *J*(PtB) ≈ 490], −3.9 (1 B), −8.0 (2 B), −10.4 (2 B), −16.6 (2 B), −23.5 (1 B)	[e] 25.4 [br, *J*(PtP) = 2141], 24.3 [*J*(PtP) = 5060]
5	18.1 [1 B, B–H⟶Pt, *J*(HB) = 60], −1.9 (1 B), −8.8 (2 B), −12.5 (2 B), −18.3 (2 B), −19.9 (1 B)	39.1 [*J*(PtP) = 3798]
6a	35.9 [d, 1 B, B–Pt, *J*(PB) = 65, *J*(PtB) ≈ 530], 1.3 (1 B), −1.0 (1 B), −2.8 (1 B), −6.7 (1 B), −16.1 (2 B), −19.3 (1 B), −20.0 (1 B)	[f] 8.00 [br, *J*(PtP) = 2148], −7.4 [*J*(PtP) = 4724]
6b	47.3 [d, 1 B, B–Pt, *J*(PB) = 76, *J*(PtB) ≈ 485], −3.6 (1 B), −7.9 (2 B), −10.3 (2 B), −16.4 (2 B), −23.3 (1 B)	[f] 11.1 [br, *J*(PtP) = 2193], −5.4 [*J*(PtP) = 5121]

[a] Chemical shifts (δ) in ppm, coupling constants (*J*) in Hz, measurements at room temperature in CD_2Cl_2, unless otherwise stated. [b] Hydrogen-1 decoupled, chemical shifts are positive to high frequency of $BF_3{\cdot}OEt_2$ (external). The B–H⟶Pt and B–Pt assignments were made from fully coupled ^{11}B spectra. [c] Hydrogen-1 decoupled, chemical shifts are positive to high frequency of 85% H_3PO_4 (external). Peaks denoted as broad have $\nu_{1/2}$ = 200–250 Hz. [d] Measured at −73 °C. [e] Measured at −90 °C. [f] Measured at −80 °C.

Table 4 Selected internuclear distances (Å) and angles (°) for the cation of [3,3,3-$(CO)_3$-3,8-(Pt{$Ph_2P(CH_2)_2PPh_2$})-8-(μ-H)-*closo*-3,1,2-$ReC_2B_9H_{10}$][BF_4] **2b**

Pt–P(1)	2.252(4)	Pt–P(2)	2.268(4)	Pt–B(4)	2.34(2)	Pt–Re	2.8126(10)
Re–C(4)	1.56(3)	Re–C(3)	1.92(3)	Re–C(5)	1.96(2)	Re–B(4)	2.29(2)
Re–B(5)	2.33(2)	Re–C(2)	2.335(13)	Re–B(3)	2.34(2)	Re–C(1)	2.35(2)
P(1)–C(6)	1.83(2)	P(2)–C(7)	1.832(14)	C(3)–O(3)	1.16(3)	C(4)–O(4)	1.41(3)
C(5)–O(5)	1.11(2)	C(6)–C(7)	1.50(2)				
P(1)–Pt–P(2)	84.6(2)	B(3)–Re–Pt	77.4(4)	C(3)–Re–Pt	74.8(5)	B(4)–Pt–Re	51.9(5)
P(1)–Pt–Re	166.95(11)	O(4)–C(4)–Re	176(2)	B(5)–Re–Pt	86.7(4)	C(3)–Re–C(5)	82.8(7)
C(4)–Re–C(3)	106.7(10)	P(1)–Pt–B(4)	115.2(6)	C(1)–Re–Pt	123.3(5)	C(5)–Re–Pt	143.1(5)
C(4)–Re–Pt	77.7(7)	P(2)–Pt–Re	108.42(12)	O(5)–C(5)–Re	176(2)	C(2)–Re–Pt	118.1(4)
B(4)–Re–Pt	53.4(4)	C(4)–Re–C(5)	81.3(9)	P(2)–Pt–B(4)	159.8(5)	O(3)–C(3)–Re	179(2)

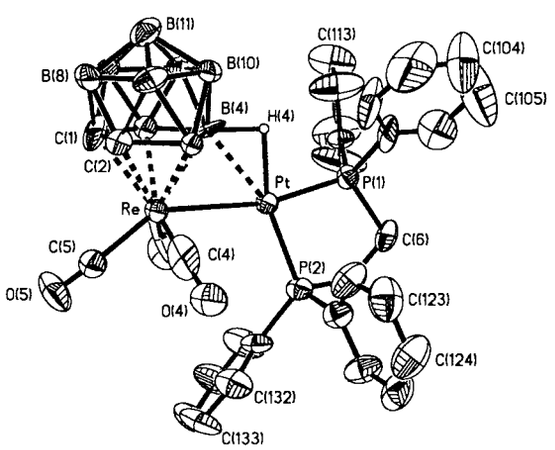

Fig. 1 Structure of the cation of [3,3,3-$(CO)_3$-3,8-(Pt{$Ph_2P(CH_2)_2$-PPh_2})-8-(μ-H)-*closo*-3,1,2-$ReC_2B_9H_{10}$][BF_4] **2b**, showing the crystallographic labeling scheme. Thermal ellipsoids are shown at the 40% probability level. Only the agostic hydrogen atom is shown for clarity.

cation is shown in Fig. 1 and salient bond lengths and angles are given in Table 4.

The Re–Pt bond [2.8126(10) Å] is slightly longer than that found in the neutral complex [2,2,2-$(CO)_3$-2,7-{$Pt(PPh_3)_2$}-7-(μ-H)-*closo*-2,1-$ReCB_{10}H_{10}$] [2.7931(4) Å],[2] suggesting that the molecular charge has little influence on this connectivity. The presence of the β-B–H⟶Pt linkage is substantiated [B(4)–Pt 2.34(2) Å] with the agostic hydrogen atom located. The corresponding distance observed in [2,2,2-$(CO)_3$-2,7-{$Pt(PPh_3)_2$}-7-(μ-H)-*closo*-2,1-$ReCB_{10}H_{10}$] is 2.355(3) Å. The distortion of the $Re(CO)_3$ unit from a tripodal piano stool arrangement found in the anion of **1** is perceptible with C(3)–Re–C(4) 106.7(10), C(3)–Re–C(5) 82.8(7) and C(4)–Re–C(5) 81.3(9)°, *i.e.* the first exceeds the last two by more than 20°. Comparison should be made with the complexes [3,3,3-$(CO)_3$-3,8-{$M(PPh_3)$}-8-(μ-H)-*closo*-3,1,2-$ReC_2B_9H_{10}$] (M = Cu or Ag) where the OC–Re–CO angles bisected by the ReMP plane are no greater than 10° more obtuse than the remaining two OC–Re–CO angles of each of those complexes.[4] In both the copper and silver complexes only one phenyl group of the $M(PPh_3)$ unit is disposed towards the $Re(CO)_3$ group. The likely cause of this enhanced perturbation in **2b** is the steric pressure from both the lower phenyl groups of the $Ph_2P(CH_2)_2PPh_2$ ligand (Fig. 1) which are forced to flank the Re–Pt bond, driving the C(3)O(3) and C(4)O(4) ligands further apart and therefore closer to the C(5)O(5) group.

When complex **2b** is dissolved in MeCN it immediately affords [$Pt(NCMe)_2${$Ph_2P(CH_2)_2PPh_2$}][3,3,3-$(CO)_3$-*closo*-3,1,2-$ReC_2B_9H_{11}$][BF_4], hence the importance of removing all traces of MeCN when isolating **2b**, usually by washing with copious quantities of Et_2O. The behaviour of complex **2b** in THF (tetrahydrofuran), however, is at variance with its simple dissociation in MeCN. This phenomenon will be analysed later pending discussion of the results of treating **2b** with various strong bases.

Solutions of complex **2b** in CH_2Cl_2 or THF were treated with various strong bases under the conditions listed in Table 5. It should be noted that the sterically encumbered reagents Proton Sponge [1,8-bis(dimethylamino)naphthalene] and DBU (1,8-diazabicyclo[5.4.0]undec-7-ene) instigated complete dissociation of the platinum fragment from the anion [3,3,3-$(CO)_3$-*closo*-3,1,2-$ReC_2B_9H_{11}$]$^-$, as did solutions of $Na[BH_4]$ (entries 1–3).

Table 5 Reaction of the salt **2b** with base under varying conditions

Entry	Base	Solvent	*T*/°C	Ratio **3a** : **3b**[a]
1	Proton Sponge	CH_2Cl_2	−80	dissoc.
2	DBU	CH_2Cl_2	−80	dissoc.
3	$Na[BH_4]$	CH_2Cl_2	−80	dissoc.
4	K-Selectride	CH_2Cl_2	−80	2 : 1
5	K-Selectride	THF	−80	1 : 1
6	LiPh	THF	−80	2 : 3
7	$LiBu^t$	THF	−80	1 : 3
8	$LiBu^t$	THF	25	1 : 4

[a] dissoc. denotes complete dissociation of the platinum fragment from the rhenacarborane fragment.

Clearly the bridged Re–Pt system of **2b** is sensitive to even mildly nucleophilic species. However, careful treatment with K-Selectride $K[BHBu^s_3]$ in CH_2Cl_2 at −80 °C (Table 5, entry 4) gave a mixture of two isomeric complexes [3,3,3-$(CO)_3$-3,*n*-(Pt{$Ph_2P(CH_2)_2PPh_2$})-*closo*-3,1,2-$ReC_2B_9H_{10}$] **3a** (*n* = 4), **3b** (*n* = 8) which were separable by column chromatography. The

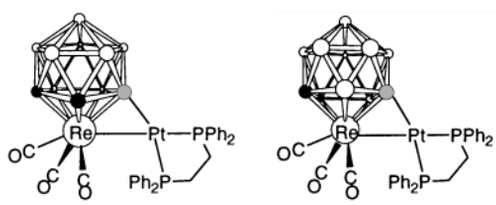

3a **3b**

species **3a** and **3b** shared almost identical IR spectra (Table 1). Microanalyses confirmed that these were isomers of the same basic molecular formula, although complex **3b** was decidedly more soluble than **3a** in CH_2Cl_2 solutions. The ^1H and ^{13}C-{^1H} NMR spectra displayed all the expected signals for the cage, CO and $Ph_2P(CH_2)_2PPh_2$ ligands for **3a** and **3b** with the exception of the CO signals for **3b** which appear as a single broad unresolved peak. The ^{11}B-{^1H} NMR spectra are particularly informative with singlet resonances at δ 37.7 (**3a**) and 49.6 (**3b**), lying isolated in the low field region away from the remaining peaks. Additionally, these signals, which both bear broad ^{195}Pt satellites [*J*(PtB) ≈ 485 (**3a**) and 440 Hz (**3b**)], remain as singlets in the fully coupled ^{11}B NMR spectrum. This is indicative of the presence of exopolyhedral B–Pt σ bonds in both **3a** and **3b**.[7a–c,8] The ^{11}B-{^1H} NMR spectrum of **3a** reveals a 1 : 1 : 1 : 1 : 1 : 2 : 2 pattern of peaks synonymous with the absence of any formal molecular symmetry. The corresponding pattern for **3b** is 1 : 1 : 2 : 2 : 2 : 1 suggesting the presence of a molecular plane of symmetry through the Re, Pt, the apical B and both P atoms. This information enabled **3a** to be assigned as the α isomer, where an α-B atom in the C$\overline{CBBB}$ ring participates in σ bonding to the platinum, and likewise **3b** as the β isomer. The ^{31}P-{^1H} NMR spectra of **3a** and **3b** display interesting features. Signals at δ 64.8 (**3a**) and 65.4 (**3b**) are broad ($\nu_{1/2}$ ≈ 220 and 250 Hz, respectively) most likely due to the *transoid* location of these P atoms with respect to the σ-bonded quadrupolar boron atoms.[2,5,7,8] Their ^{195}Pt–^{31}P coupling constants [*J*(PtP) = 2060 (**3a**) and 2050 Hz (**3b**)] are diminished by *ca.* 1300 Hz in comparison with the corresponding signal for **2b** [δ 55.9, *J*(PtP) = 3393 Hz]. Furthermore, the P nuclei *transoid* to the Re–Pt bonds resonate at δ 48.0 (**3a**) and 49.0 (**3b**) with *J*(PtP) values which are *ca.* 1750 and 2200 Hz, respectively, greater than that in complex **2b** [δ 62.3, *J*(PtP) = 2955 Hz] (Table 3). The implication is that upon deprotonation of the agostic B–H⟞Pt bridge with formation of a B–Pt bond the B-*transoid* phosphorus atom of the phosphine arm becomes more weakly bound, while the Re-*transoid* P atom (*cisoid* to B) becomes more strongly bonded. This inference is based on the premise that ^{195}Pt–^{31}P one-bond coupling constants are sensitive to the

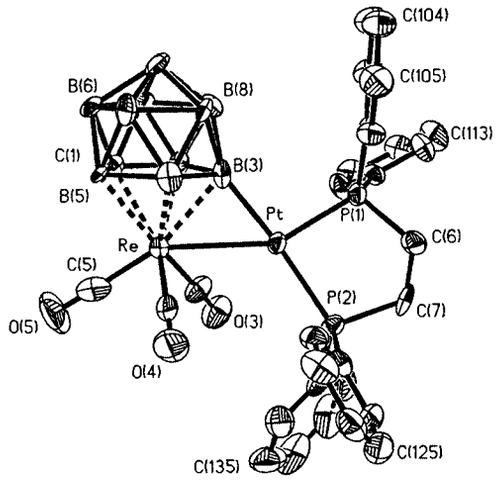

Fig. 2 Structure of [3,3,3-$(CO)_3$-3,4-(Pt{$Ph_2P(CH_2)_2PPh_2$})-*closo*-3,1,2-$ReC_2B_9H_{10}$] **3a**, showing the crystallographic labeling scheme. Thermal ellipsoids are shown at the 40% probability level. Hydrogen atoms are omitted for clarity.

Pt–P bond distances.[9] To test this notion, single crystals of **3a** were grown for the purpose of carrying out an X-ray diffraction study. Selected bond lengths and angles are given in Table 6 and the structure is shown in Fig. 2.

The $Re(CO)_3$ unit is less distorted from a pseudo-symmetrical piano stool arrangement [C(3)–Re–C(4) 93.5(7), C(3)–Re–C(5) 84.5(8), C(4)–Re–C(5) 85.7(7)°] than in complex **2b**, most likely because the Pt{$Ph_2P(CH_2)_2PPh_2$} fragment has been lifted away from the $Re(CO)_3$ moiety upon completion of the conversion from the B–H⟞Pt system to the B–Pt σ bond. This process involves an effective contraction of the B–Pt distance from 2.34(2) Å [Pt–B(4) in **2b**] to 2.061(18) Å [Pt–B(3) in **3a**]. The disparity between Pt–P bond lengths in **3a** is evident with the Pt–P(1) bond [2.202(4) Å] *transoid* to the Re atom shorter than that in **2b** [2.252(4) Å] and the Pt–P(2) bond [2.314(4) Å] *transoid* to the α-B atom longer than in **2b** [2.268(4) Å]. While neither structure is of exemplary quality, making it necessary to treat the data with a little caution, the comparisons would seem to support the NMR evidence discussed above. Thus the σ-bonded carbaborane cage might be considered to exert a considerably stronger *trans* influence on a Pt–P bond than a B–H⟞ moiety, which would be expected when it is recalled that σ effects are most significant when evaluating *trans* influences.[9] The shorter Pt–P(1) bond in complex **3a** as compared with that in **2b** may be accounted for by the decrease in positive charge on the platinum, leading to increased π back donation to both phosphine ligands. This effect is more than offset for the Pt–P(2) bond in **3a** by the *trans* influence exerted by the B–Pt σ bond. It should be noted that similar features for the ^{195}Pt–^{31}P NMR coupling constants and the Pt–PEt_3 bond lengths were reported for the complex [1,2-Me_2-3-(μ-H)-3,3-$(CO)_2$-3-(PMe_3)-3,4-{$Pt(PEt_3)_2$}-8-($CH_2C_6H_4$Me-4)-*closo*-3,1,2-$WC_2B_9H_7$], which has a B–Pt bond *trans* to one phosphine and *cis* to another, though these properties were not previously discussed.[5]

One curious aspect of the reaction of complex **2b** with K-Selectride in CH_2Cl_2 at −80 °C is how the majority of the product formed could be the α isomer **3a** (by a ratio of 2 : 1 over **3b**) when the starting material exists solely as the β isomer. The product distribution would seem to rule out a simple acid–base exchange where the Selectride anion abstracts a proton from the B–H⟞Pt group. It is more likely that the Selectride delivers a hydride anion to the platinum center, where most of the cationic charge of **2b** logically resides (Scheme 1). This might be accompanied by the displacement of one of the phosphine ligand P atoms, giving a neutral intermediate $\mathbf{A}_\beta$ with a terminal hydride. Support for such a structure will be presented later when compound **5** is discussed. It is at this point that isomeriz-

Table 6 Selected internuclear distances (Å) and angles (°) for [3,3,3-$(CO)_3$-3,4-(Pt{$Ph_2P(CH_2)_2PPh_2$})-*closo*-3,1,2-$ReC_2B_9H_{10}$] **3a**

Pt–B(3)	2.061(18)	Pt–P(1)	2.202(4)	Pt–P(2)	2.314(4)	Pt–Re	2.7583(9)
Re–C(4)	1.89(2)	Re–C(5)	1.93(2)	Re–C(3)	1.95(2)	Re–B(3)	2.28(2)
Re–C(1)	2.296(14)	Re–C(2)	2.307(14)	Re–B(5)	2.373(14)	Re–B(4)	2.39(2)
C(3)–O(3)	1.15(2)	C(4)–O(4)	1.18(2)	C(5)–O(5)	1.18(2)		
B(3)–Pt–P(1)	97.0(4)	B(5)–Re–Pt	119.3(4)	C(5)–Re–Pt	147.9(6)	P(2)–Pt–Re	122.29(10)
B(3)–Pt–Re	54.2(4)	O(4)–C(4)–Re	176(2)	C(1)–Re–Pt	117.8(3)	C(5)–Re–C(3)	84.5(8)
C(4)–Re–C(5)	85.7(7)	B(3)–Pt–P(2)	173.4(4)	B(4)–Re–Pt	78.2(4)	C(3)–Re–Pt	67.2(5)
C(4)–Re–Pt	81.6(5)	P(1)–Pt–Re	150.75(11)	O(5)–C(5)–Re	177(2)	C(2)–Re–Pt	79.4(3)
B(3)–Re–Pt	47.1(4)	C(4)–Re–C(3)	93.5(7)	P(1)–Pt–P(2)	86.9(2)	O(3)–C(3)–Re	174.6(14)

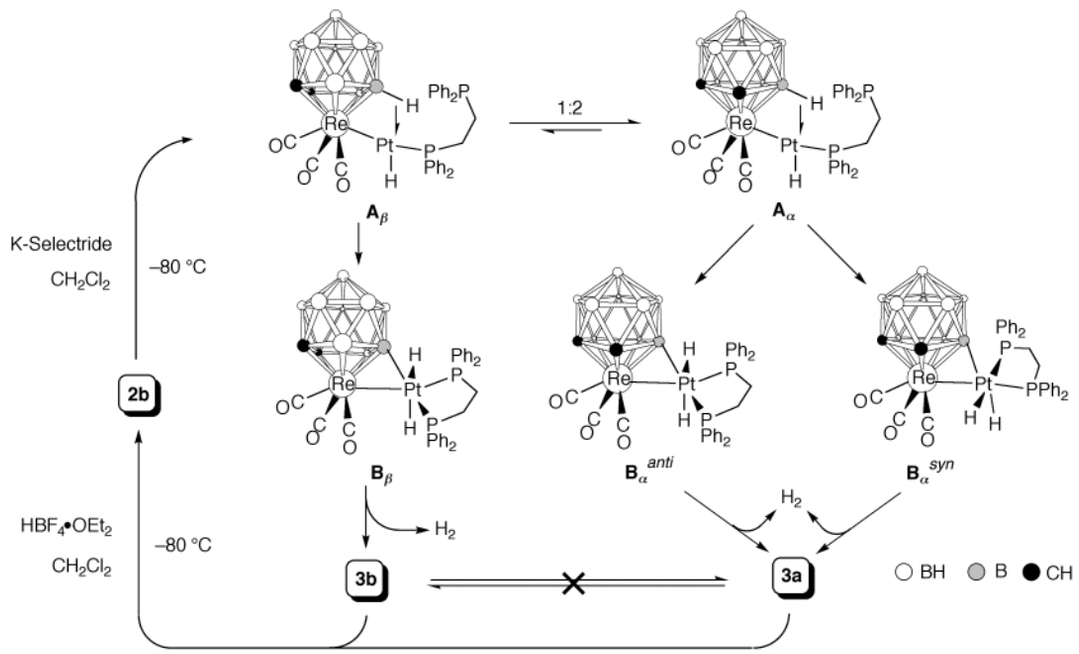

Scheme 1 Possible pathways in the formation of complexes **3a** and **3b** by addition of K-Selectride to **2b** in CH_2Cl_2 at low temperature.

ation to $\mathbf{A}_\alpha$ can occur, since there clearly is no such rearrangement in the starting material **2b**. This would involve a transformation from the β-B–H⟶Pt to the α-B–H⟶Pt system, which has previously been reported for several related molecules having B–H⟶M groups,[2,10] and it is here that $\mathbf{A}_\alpha$ would be favoured over $\mathbf{A}_\beta$ by a ratio of 2:1. A dual pathway may then swing into operation with both molecules $\mathbf{A}_\alpha$ and $\mathbf{A}_\beta$ undergoing oxidative addition reactions of their B–H⟶Pt groups to give B–Pt–H systems. The platinum(IV) centers so generated in the intermediates $\mathbf{B}_\alpha^{anti}$ (or $\mathbf{B}_\alpha^{syn}$) and $\mathbf{B}_\beta$ can be stabilized by recoordination of the pendant phosphine arm in a *trans* position with respect to the newly generated hydride ligand. The isomers $\mathbf{B}_\alpha^{anti}$ and $\mathbf{B}_\alpha^{syn}$ arise from the fact that there would be two enantiomeric forms of $\mathbf{A}_\alpha$ and the second hydride in $\mathbf{B}_\alpha$ could lie *anti* or *syn* to the cage carbon atoms. Now the hydrogen atoms of the PtH_2 group are suitably located in a *cisoid* fashion to undergo reductive elimination processes to give the observed products **3a** and **3b**. Such oxidative addition–reductive elimination processes involving exopolyhedral platinum fragments on metallacarbaborane cages are well documented.[5,7a–c,8]

Both **3a** and **3b** can be protonated with HBF_4·OEt_2 to regenerate complex **2b** quantitatively. Reverse α ⟶ β isomerization must therefore occur in the conversion of **3a** into **2b**. In an attempt to make a closer examination of the protonation of **3a**, a sample was dissolved in CD_2Cl_2 in an NMR tube and cooled to −80 °C in the spectrometer probe, then removed briefly to treat it with 1 mol equivalent of HBF_4·OEt_2. A ^1H NMR spectrum run at −80 °C within a few seconds of reintroducing the sample displayed a weak apparent triplet at δ −16.4 [J(PH) = 7 and 7 Hz]. A further weaker broad resonance was observed at δ −19.2 and the ratio of these signals was 3:1 respectively. The peaks were too weak to be able to observe ^{195}Pt satellites. When the sample is warmed these signals are seen to broaden and disappear as conversion into **2b** is completed. We attribute these signals to the cationic species $\mathbf{C}_\alpha$ (Scheme 2) where the Pt atoms

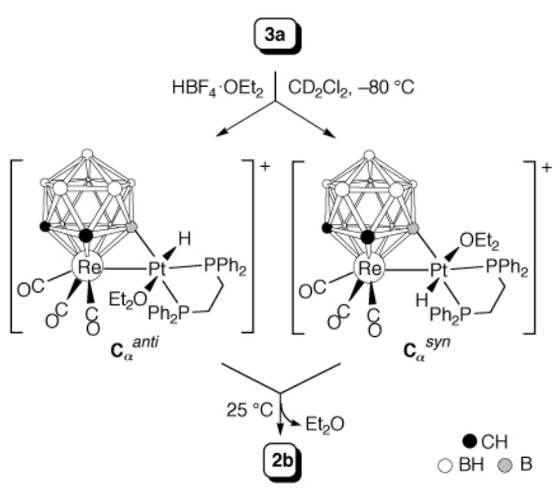

Scheme 2 Protonation of complex **3a** to reform salt **2b**.

bear terminal hydride ligands *cisoid* to both the phosphorus nuclei. These structures can be appreciated by considering that the platinum d_{z^2} orbital in **3a** is the most conceivable site for attack by H^+. Rehybridization of the platinum center upon increase in formal oxidation number (Pt^{II} ⟶ Pt^{IV}) could be accompanied by coordination and stabilization by Et_2O,

conveniently delivered with the acid reagent and necessarily bonded *trans* to the hydride ligand. Depending on which side of the molecule the acid attacked, two isomers are possible (*syn* and *anti*), though identification of the major species is, however, indeterminable. In both $\mathbf{C}_{\alpha}^{syn}$ and $\mathbf{C}_{\alpha}^{anti}$ the hydride is in position (*cisoid* to the α-boron) to undergo formation of an α-B–H⟶Pt group by reductive elimination and concomitant loss of Et_2O to give **2a**. Instantaneous rearrangement to give the β-B–H⟶Pt group would alternatively yield **2b**.

The behavior of salt **2b** in THF was alluded to above and revealed to be unlike that in MeCN where complete dissociation occurred. In fact in d_8-THF the complex is present in its cationic form at a level of only *ca.* 20%. The remainder was identified as a mixture of the complexes **3a** and **3b** in a ratio of 1:3. Thus THF itself is capable of acting as a deprotonating agent setting up an equilibrium mixture of **2b**, **3a** and **3b**. To support this a ^{1}H NMR spectrum of a d_8-THF sample showed a broad peak at δ 10.88 which corresponds with that for solutions of protonated THF molecules, $[C_4H_8OH]^+$, as shown by treating a sample of d_8-THF with a small amount of $HBF_4{\cdot}OEt_2$. The mechanism of the THF deprotonation is most likely similar to that described in Scheme 1, except that cationic intermediates are involved where THF is bound to the Pt atoms (Scheme 3). The first of these to form could be $\mathbf{D}_{\beta}$, akin to $\mathbf{A}_{\beta}$

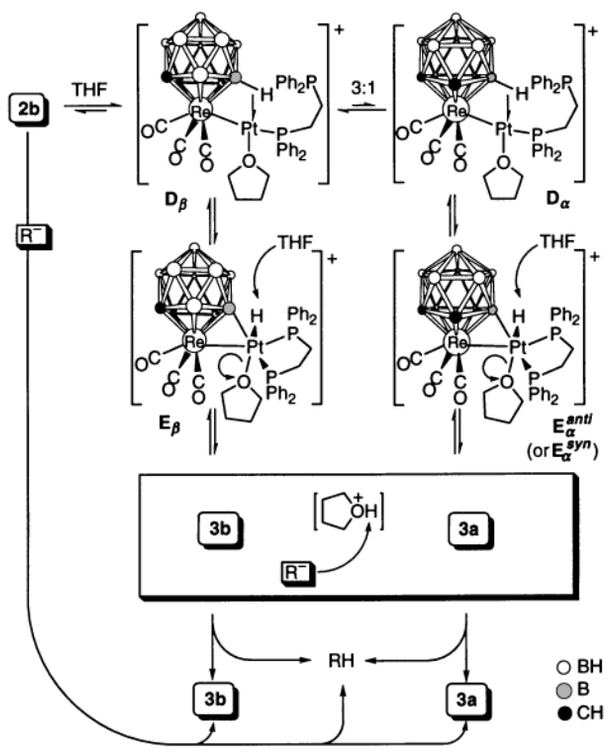

Scheme 3 THF as a base in the formation of complexes **3a** and **3b** from **2b**.

(and to complex **5** discussed presently). An exchange might then occur between $\mathbf{D}_{\beta}$ and $\mathbf{D}_{\alpha}$, though under these conditions the former β isomer is favored, accounting for the higher percentage of **3b** in the mixture. The intermediates **E** as shown bear resemblance to **B** (Scheme 1) and also to **C** (Scheme 2), noting that the THF molecules in **E** would be situated *trans* to the cage boron atom. The $\mathbf{D}_{\alpha}/\mathbf{D}_{\beta}$ equilibrium would go some way to explaining why most of the deprotonations with strong bases in THF (Table 5, entries 5–8) result in a product distribution favouring **3b** over **3a**. Most of the base (R^-) merely abstracts H^+ from the protonated THF molecule, though some will still react with the small amount of **2b** present in THF solution. Hence the outcome of the reactions in Table 5 (entries 5–8) is dictated as much by the solvent used as the strong base added.

Reactions between complex **1** and other platinum–phosphine combinations $[Pt(NCMe)_2(PR_3)_2][BF_4]_2$ [$PR_3 = PEt_3$, $(PR_3)_2 = (C_6H_{11})_2P(CH_2)_2P(C_6H_{11})_2$] proved too difficult to work up to give pure products. To circumvent this the salt **1** was treated with $[Pt(H)(THF)(PEt_3)_2][BF_4]$, readily generated *in situ* from $[PtCl(H)(PEt_3)_2]$ and $Ag[BF_4]$ in THF. This procedure has the advantage of pre-equipping the platinum fragment with a hydrogen atom, so that the product might be expected to be both neutral and lead to the elimination of molecular hydrogen. When the reaction was carried out in refluxing THF for 4 d (Scheme 4) two neutral products were indeed isolated after

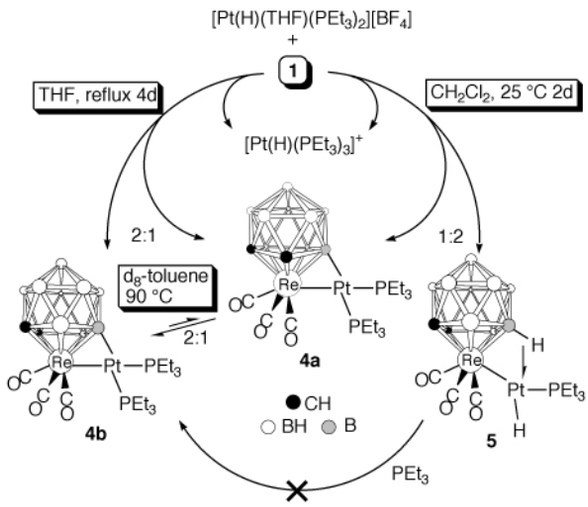

Scheme 4 Reactions of salt **1** with $[Pt(H)(THF)(PEt_3)_2][BF_4]$ under differing conditions.

chromatographic purification, [3,3,3-$(CO)_3$-3,*n*-{$Pt(PEt_3)_2$}-*closo*-3,1,2-$ReC_2B_9H_{10}$] **4a** ($n = 4$), **4b** ($n = 8$), in a ratio of 1:2, respectively. The yields (Table 1) of both were poor and it should be noted that the synthesis of **4a** and **4b** was accompanied by the formation of significant amounts of the cation $[Pt(H)(PEt_3)_3]^+$. This was identified from the ^{1}H and ^{31}P-{^{1}H} NMR spectra of the reaction mixture but not isolated.

The IR spectra (Table 1) of both complexes **4a** and **4b** are very similar to those of **3a** and **3b**, respectively, immediately suggesting analogous structures. The ^{11}B-{^{1}H} NMR spectrum (Table 3) of **4a** contains a diagnostic doublet resonance with broad ^{195}Pt satellites at δ 34.5 [J(PB) = 76, J(PtB) ≈ 580 Hz] to be compared with the corresponding signal in the same spectrum of **3a** [δ 37.7, J(PtB) ≈ 485 Hz]. The signal for **4a** remains unchanged in a fully coupled ^{11}B NMR spectrum, confirming the presence of a B–Pt linkage. Likewise the ^{11}B-{^{1}H} NMR spectrum of **4b** displays a peak at δ 45.6 [J(PtB) ≈ 490 Hz] to be compared with that of **3b** [δ 49.6, J(PtB) ≈ 440 Hz]. The ^{1}H and ^{13}C-{^{1}H} NMR spectra were also supportive of the proposed structures, though it was necessary to carry out data accumulations at low temperatures (–73 °C for **4a** and −90 °C for **4b**). The ^{13}C-{^{1}H} NMR spectra showed three CO resonances for **4a** [δ 196.9, 192.7, 191.7 (1:1:1)] reflecting the lack of symmetry in the molecule, and two for **4b** [δ 197.2, 191.0 (1:2)] as a result of the molecular C_s symmetry, a plane encompassing the Re, Pt, apical B and P atoms. The peaks in the ^{31}P-{^{1}H} NMR spectra of **4a** and **4b** measured at room temperature were perceptibly broader than their counterparts in the spectra of **3a** and **3b**. Running the spectral measurements at −70 and −80 °C, respectively, led to more discernible signals (Table 3) which were now similar to those of **3a** and **3b** at room temperature, especially in terms of the wide disparity between the ^{195}Pt–^{31}P coupling constants of the two phosphorus nuclei in any one species. Apparently the onset of some dynamic process is being observed at room temperature (see below).

Repeating the reaction of **1** with $[Pt(H)(THF)(PEt_3)_2][BF_4]$ but in CH_2Cl_2 at ambient temperatures yielded complex **4a** and a second compound which was easily separated by chromatographic purification and fractional crystallization. This second species was identified as $[3,3,3\text{-}(CO)_3\text{-}3,8\text{-}\{Pt(H)(PEt_3)\}\text{-}8\text{-}(\mu\text{-}H)\text{-}closo\text{-}3,1,2\text{-}ReC_2B_9H_{10}]$ **5** and the ratio of **4a**:**5** was found to be 1:2. There was no evidence of the formation of **4b** under these conditions. Compound **5** was easily identified from physical and spectroscopic data (Tables 1–3). The ^1H NMR spectrum displays two notable high field resonances. The first at δ −4.84 shows the distinctive characteristics of a B–H⟶Pt system with $J(BH) = 60$ Hz and satellites due to the ^{195}Pt nucleus [$J(PtH) \approx 465$ Hz].[5,7] An additional doublet splitting [$J(HH) = 15$ Hz] results from a *trans* coupling across the platinum with a terminal hydride, which gives rise to the second high field resonance at δ −11.03. The latter signal is quite broad with irresolute ^{31}P–^1H or ^1H–^1H couplings, but with a large ^{195}Pt–^1H coupling for the satellites [$J(PtH) = 1090$ Hz], strongly indicating the terminal nature of this hydride ligand.[7a,11] This is reminiscent of the complex $[1,2\text{-}Me_2\text{-}3\text{-}(\mu\text{-}CC_6H_3Me_2\text{-}2,6)\text{-}3,3\text{-}(CO)_2\text{-}3,8\text{-}\{Pt(PEt_3)\}\text{-}8\text{-}(\mu\text{-}H)\text{-}closo\text{-}3,1,2\text{-}WC_2B_9H_8]$ which has a terminal platinum hydride [δ −10.22, $J(PtH) = 1165$ Hz] and a *trans* B–H⟶Pt proton (δ −4.7), though the ^1H NMR spectrum from which these resonances were taken lacks the fine detail observed for that of complex **5**.[7a] The employment of the β-B atom (CCB*B*B) in the B–H⟶Pt agostic system is evident from the ^1H, $^{13}C\text{-}\{^1H\}$ and $^{11}B\text{-}\{^1H\}$ NMR spectra (Tables 2 and 3). The first of these shows a single resonance for the cage CH protons (δ 3.42), implying the presence of a mirror plane bisecting the molecule which would not be associated with the use of a boron atom α to the cage carbons in the CC*B*BB ring. This is supported by the signal count in the $^{11}B\text{-}\{^1H\}$ NMR spectrum and their integrals (1:1:2:2:2:1). The peak at δ 18.1 in this spectrum is in the region expected for B–H⟶Pt groups with a diagnostic ^1H–^{11}B coupling [$J(HB) = 60$ Hz].[5,7] The presence of only one PEt_3 ligand on the platinum was realized in the $^{31}P\text{-}\{^1H\}$ NMR spectrum (Table 3) with a single sharp resonance at δ 39.1 [$J(PtP) = 3798$ Hz] and particularly in the ^1H NMR spectrum where peak integrals were particularly informative. The 15 Hz coupling between the agostic and terminal hydrogen nuclei was verified by a ^1H NMR measurement with selective decoupling of the broad hydride resonance at δ −11.03 (Supporting Information). With the exception of the satellites, the doublet of quartets at δ −4.84 was reduced to a simple ^{11}B-coupled quartet, as expected.

Thus the loss of a PEt_3 ligand is confirmed in the formation of complex **5**, the structure of which would seem to support the postulated intermediates **A** in Scheme 1, and perhaps even **D** in Scheme 3. Phosphine dissociation would also be consistent with the observed formation of the $[Pt(H)(PEt_3)_3]^+$ cation. Since the product ratio of **4a**:**5** (1:2) matches that of **4a**:**4b** (1:2) it might have been expected that **5** was in fact the logical precursor to **4b**, noting that in their exopolyhedral interactions with the platinum atom both involve β-B vertices. It was further thought that addition of 1 mol equivalent of PEt_3 to **5** would afford **4b**. However, this did not occur (Scheme 4). An NMR examination of the reaction mixture revealed a *ca.* 50% decomposition of **5** to $[Pt(H)(PEt_3)_3][3,3,3\text{-}(CO)_3\text{-}closo\text{-}3,1,2\text{-}ReC_2B_9H_{11}]$. The question then arises as to how **4b** forms and perhaps, therefore, a shadow of doubt is thrown on the intermediacy of **A** (Scheme 1) in the synthesis of the compounds **3**. It was previously mentioned that **4a** and **4b** may be undergoing some dynamic process at room temperature (see above). NMR spectra were measured on a sample of **4a** in d_8-toluene at 90 °C, as it was suspected that spectral measurements at an elevated temperature would reveal something about this dynamic process. To our great surprise the formation of **4b** was clearly observed to occur until a ratio of **4a** to **4b** of 1:2 was reached, this taking *ca.* 3 h at this temperature. A similar result was obtained when starting with a sample of **4b**. It is therefore merely a coincidence that the CH_2Cl_2 reaction at room temperature between **1** and $[Pt(H)(THF)(PEt_3)_2][BF_4]$ (Scheme 4) produces **4a** and **5** in a ratio of 1:2. The formation of **4b** can solely be accounted for by the isomerization of **4a** at a temperature as low as that of refluxing THF (65 °C).

We have synthesized many dimetallic carbaborane complexes where one of the metals is exopolyhedrally σ bonded to a boron atom in the CCBBB ring of a $1,2\text{-}R_2\text{-}closo\text{-}3,1,2\text{-}MC_2B_9H_8$ (R = H or Me) cage.[12] Hitherto there has been no precedent in this chemistry for σ-bonded *exo*-metal fragments isomerizing in such a manner as to transfer from α-B to β-B vertices, or *vice versa*. There was not even any evidence of such exchange occurring between complexes **3a** and **3b** in this study.

To account for the broadness of the peaks in the NMR spectra of complexes **4a** and **4b** at ambient temperatures a dynamic process involving heterolytic Re–Pt bond cleavage may be taking place. This would be feasible because the local $Re(CO)_3$ moiety is perfectly stable in *exo-closo* complexes such as $[3,3,3\text{-}(CO)_3\text{-}8\text{-}(\mu\text{-}H)\text{-}8\text{-}\{M(CO)_2(\eta\text{-}C_5H_5)\}\text{-}closo\text{-}3,1,2\text{-}ReC_2B_9H_{10}]$ (M = Fe or Ru) and $[3,3,3\text{-}(CO)_3\text{-}8,9,12\text{-}(\mu\text{-}H)_3\text{-}8,9,12\text{-}\{RuCl(PPh_3)_2\}\text{-}closo\text{-}3,1,2\text{-}ReC_2B_9H_8]$[4] as it is in the parent anion of **1**. The cationic platinum center of the pendant *exo*-$[Pt(PEt_3)_2]^+$ group could readily be stabilized by the adjacent β-B–H bond (starting from **4a**) or one of the two available α-B–H bonds (starting from **4b**) to give zwitterionic intermediates $\mathbf{F}_\alpha$ or $\mathbf{F}_\beta$, respectively (Scheme 5). Interconversion processes involving

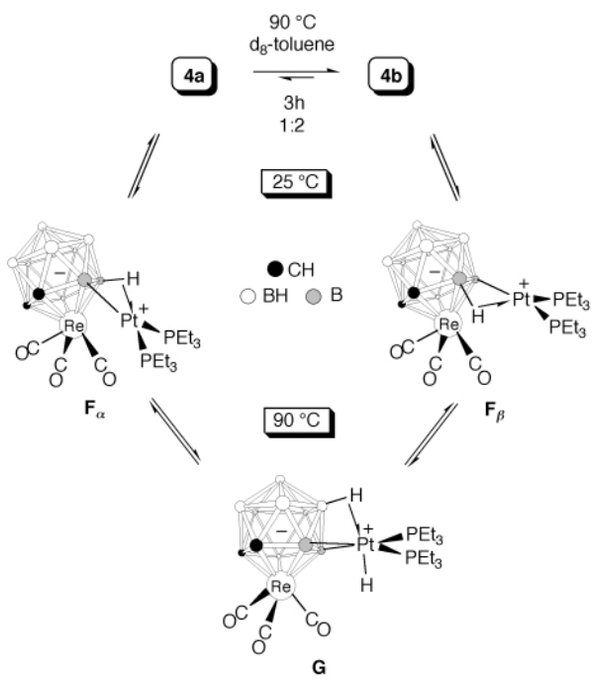

Scheme 5 Possible mechanism for the interconversion between isomers **4a** and **4b**.

metal–metal bond fission/formation and which give such *exo-closo* species with no M–M connectivity have been documented for solutions of the complexes $[3,3,3\text{-}(CO)_3\text{-}8,9\text{-}(\mu\text{-}H)_2\text{-}8,9\text{-}\{Rh(PPh_3)_2\}\text{-}closo\text{-}3,1,2\text{-}ReC_2B_9H_9]$ and $[3,3,3\text{-}(CO)_3\text{-}3,8\text{-}\{M(PPh_3)\}\text{-}8\text{-}(\mu\text{-}H)\text{-}closo\text{-}3,1,2\text{-}ReC_2B_9H_{10}]$ (M = Cu or Ag).[4] At elevated temperatures (in refluxing THF or above) a full oxidative addition of the α- or β-B–H bond might occur to give a platinum(IV) center. In the resulting intermediate **G** this more electrophilic Pt atom could be stabilized by a B–H bond from the non-metal-coordinating B_5 belt. Once again this can satisfactorily be rationalized because these B_5 belt boron vertices are occasionally found to participate in agostic bonding to *exo*-metals.[4,13] Intermediate **G** may then transform into either of the

intermediates **F**, which can then undergo reformation to **4a** or **4b**. The ground-state structures for **4a** and **4b** at the low temperatures of the NMR measurements are unlikely to be in the form of **F**, as the NMR spectra are most similar to those of their **3a** and **3b** congeners. Additionally, there is no actual direct spectral evidence for the intermediates **F** or for **G**.

Doubts were raised above as to the viability of the postulated intermediates **A** and **D** in Schemes 1 and 3, since the complex **5** did not proceed to give **4b** as had been expected. An alternative system was therefore scrutinized: the reaction of **1** with the salt $[Pt(Me)(THF)(PMe_2Ph)_2][BF_4]$, generated *in situ* by treating $[PtCl(Me)(PMe_2Ph)_2]$ with 1 mol equivalent of $Ag[BF_4]$ in THF. The reaction was evidently much more rapid than that between **1** and $[Pt(H)(THF)(PEt_3)_2][BF_4]$ as a single product, $[3,3,3\text{-}(CO)_3\text{-}3,4\text{-}\{Pt(PMe_2Ph)_2\}\text{-}closo\text{-}3,1,2\text{-}ReC_2B_9H_{10}]$ **6a**, was isolated after 1 h reaction time at room temperature. Compound **6a** was characterized from spectroscopic data (Tables 2 and 3) and found to be manifestly similar to **4a**. Most notable was the doublet resonance in the $^{11}B\text{-}\{^1H\}$ NMR spectrum at δ 35.9 [J(PB) = 65, J(PtB) ≈ 530 Hz] to be compared with that in **4a** [δ 34.5, J(PB) = 76, J(PtB) ≈ 580 Hz]. The room temperature $^{31}P\text{-}\{^1H\}$ NMR spectrum for **6a** was also similar to that for **4a**, implying the existence of an analogous dynamic process and it was necessary to measure this and the ^1H and $^{13}C\text{-}\{^1H\}$ NMR spectra at −80 °C to observe distinguishable signals.

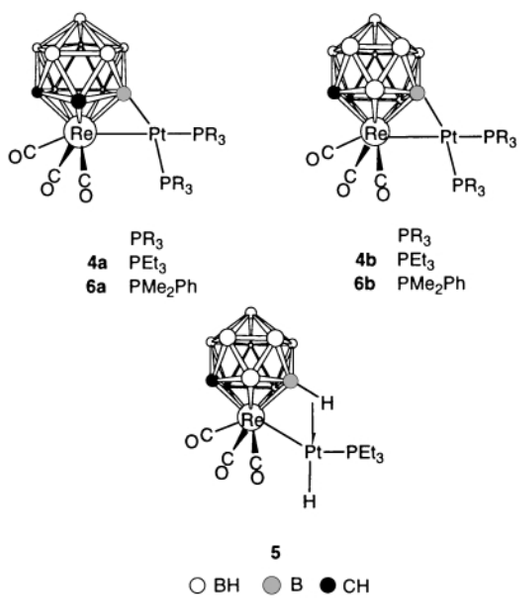

The reaction that produced complex **6a** was monitored by IR and NMR spectroscopy and after about 30 min reaction time the IR and NMR data clearly indicated the presence of a species, designated **H** (Scheme 6), akin to complex **5**. The IR spectrum of **H** showed peaks at 2034, 1964 and 1949 cm^{-1} which are almost identical with those of **5** (2034, 1962, 1950 cm^{-1}). The ^1H NMR spectrum of **H** displayed a diagnostic quartet at δ −5.07 [J(BH) = 81 Hz] with a ^{195}Pt satellite set [J(PtH) = 209 Hz], in addition to a peak at δ 0.88, where $Pt^{II}Me$ groups typically resonate.[14] Also detected in the mixture were signals due to free PMe_2Ph and the cation $[Pt(Me)(PMe_2Ph)_3]^+$, verified by independent synthesis of this species. This would support the idea of phosphine ligand dissociation from one platinum center to be scavenged by another. As the reaction proceeded beyond 30 min, IR and NMR peaks due to **H** diminished and those for **6a** grew accordingly. Thus **H**, which must possess an α-B–H⟶Pt unit, is likely to be an intermediate on the path to **6a**, and the existence of **A** and **D** in Schemes 1 and 3 is placed on a firmer footing.

Continued stirring of solutions of complex **6a** in CH_2Cl_2 for 24 h accompanied by analysis by NMR spectroscopy revealed

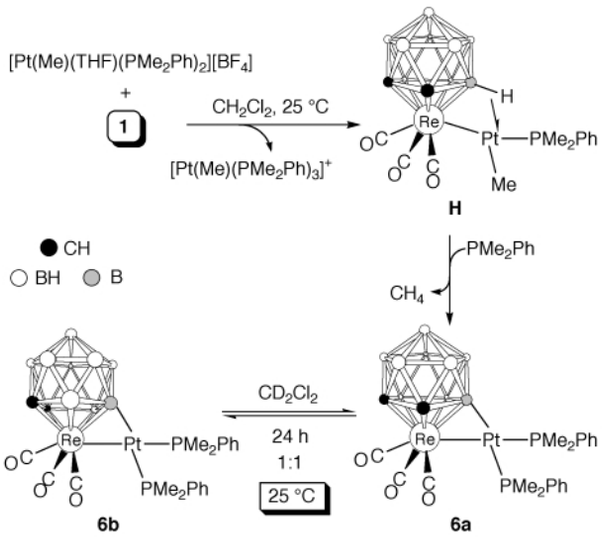

Scheme 6 Formation of complex **6a** and the facile interconversion with its isomer **6b**.

the establishment of an equilibrium with a second isomer. This was identified as $[3,3,3\text{-}(CO)_3\text{-}3,8\text{-}\{Pt(PMe_2Ph)_2\}\text{-}closo\text{-}3,1,2\text{-}ReC_2B_9H_{10}]$ **6b** from new signals that appeared in the NMR spectra of the mixture. The final equilibrium ratio of **6a** to **6b** at 25 °C was found to be 1:1 and furthermore **6b** could not be isolated free of **6a**. However, because all relevant signals for **6a** were identified from near pure solutions of this complex, those for **6b** in the mixture were easily abstracted from the spectra of the mixture. The $^{11}B\text{-}\{^1H\}$ NMR spectrum of **6b** displayed a doublet peak at δ 47.3 with the customary broad ^{195}Pt satellites [J(PB) = 76, J(PtB) ≈ 485 Hz]. These data are very close to those observed for **4b** [δ 45.6, J(PtB) ≈ 490 Hz]. The ^1H and $^{13}C\text{-}\{^1H\}$ NMR spectra measured at −80 °C both reflected the presence of an apparent mirror plane bisecting the molecule through the Re, Pt, apical B and both P atoms with one signal in the ^1H NMR spectrum at δ 3.41 for the cage CH protons and also in the $^{13}C\text{-}\{^1H\}$ NMR spectrum at δ 34.5 for the cage CH carbon nuclei. In the latter spectrum the CO nuclei give rise to two signals at δ 192.2 and 191.8 (1:2) as expected with the molecular C_s symmetry. Clearly **6b** is an analog of **3b** and **4b**. The room temperature $^{31}P\text{-}\{^1H\}$ NMR spectrum of the **6a**/**6b** mixture comprised poorly resolved peaks which became sharper at −80 °C. The same dynamic equilibrium that produced **4b** from **4a** must be occurring for the complexes **6**, except that for the latter it is an ambient temperature phenomenon, a feature entirely without precedent in this sphere of metallacarbaborane chemistry. The reason for the difference in the facility of isomeric interconversion, or lack thereof, for the compounds **3**, **4** and **6** is at the present time unknown.

Conclusion

As we expand our crop of new metallacarbaboranes incorporating $1,2\text{-}R_2\text{-}closo\text{-}3,1,2\text{-}MC_2B_9H_9$ (R = H or Me) and $closo\text{-}2,1\text{-}MCB_{10}H_{11}$ cages, it is apparent to us that our understanding of their subsequent reactivity patterns is still limited. In particular, the activation of B–H vertices in the CCBBB coordinating face of the carbaborane remains currently unpredictable. This effect is clearly dependent on the physical conditions under which it is made to occur (as in the syntheses of complexes **3**, **4** and **5**), as well as the intrinsic structure of the metallacarbaboranes (*cf.* complexes **4** and **6**).

Experimental

General

All experiments were conducted under an atmosphere of dry

nitrogen using Schlenk tube techniques. Solvents were freshly distilled under nitrogen from appropriate drying agents before use. Light petroleum refers to that fraction of boiling point 40–60 °C. Chromatography columns (*ca.* 20 cm long and 2 cm in diameter) were packed with silica gel (Acros, 60–200 mesh). Celite pads used for filtration were *ca.* 3 cm long and 2 cm in diameter. The NMR measurements were recorded at the following frequencies: ^{1}H at 360.13, ^{13}C at 90.56, ^{11}B at 115.55, and ^{31}P at 145.78 MHz. The reagents **1**,[4] $[PtCl(H)(PEt_3)_2]$,[15] and $[PtCl(Me)(PMe_2Ph)_2]$[8a] were made as previously described. The platinaphosphine complex $[PtCl_2\{Ph_2P(CH_2)_2PPh_2\}]$ was synthesized by adding $Ph_2P(CH_2)_2PPh_2$ to CH_2Cl_2 solutions of $[PtCl_2(NCPh)_2]$.[16] K-Selectride, Proton Sponge, DBU, $Na[BH_4]$ and $Ag[BF_4]$ were purchased from Aldrich.

Preparations

$[3,3,3\text{-}(CO)_3\text{-}3,8\text{-}(Pt\{Ph_2P(CH_2)_2PPh_2\})\text{-}8\text{-}(\mu\text{-}H)\text{-}closo\text{-}3,1,2\text{-}ReC_2B_9H_{10}][BF_4]$. To the compounds $[PtCl_2\{Ph_2P(CH_2)_2PPh_2\}]$ (0.40 g, 0.60 mmol) and $Ag[BF_4]$ (0.24 g, 1.23 mmol) was added MeCN (20 cm^3). A precipitate appeared almost instantaneously, though stirring was maintained for *ca.* 2 h. The suspension was filtered through a Celite pad to remove AgCl using MeCN as solvent. The volume of the filtrate was then reduced to *ca.* 5 cm^3 and a solution of **1** (0.32 g, 0.60 mmol) in MeCN (10 cm^3) added and stirred for 5 min. Solvent was then removed *in vacuo* and CH_2Cl_2 (20 cm^3) added to the residue. The suspension, now containing undissolved $CsBF_4$, was once again filtered through Celite and solvent then removed *in vacuo*. Crystallization from CH_2Cl_2–Et_2O (20 cm^3, 1:4), followed by washing with Et_2O (4 × 20 cm^3) and drying *in vacuo*, yielded $[3,3,3\text{-}(CO)_3\text{-}3,8\text{-}(Pt\{Ph_2P(CH_2)_2PPh_2\})\text{-}8\text{-}(\mu\text{-}H)\text{-}closo\text{-}3,1,2\text{-}ReC_2B_9H_{10}][BF_4]$ **2b** (0.55 g).

$[3,3,3\text{-}(CO)_3\text{-}3,n\text{-}(Pt\{Ph_2P(CH_2)_2PPh_2\})\text{-}closo\text{-}3,1,2\text{-}ReC_2B_9H_{10}]$ (n = 4 or 8). Various alkali metal bases can be used in this reaction in addition to varying the solvent between CH_2Cl_2 and THF (see text). The use of one particular base (K-Selectride) and solvent (CH_2Cl_2) is documented here. Complex **2b** (0.10 g, 0.09 mmol) was dissolved in CH_2Cl_2 (10 cm^3) and cooled to −80 °C. A solution of K-Selectride (1 M in THF, 13 μl, 0.09 mmol) was added and stirring maintained while warming to room temperature. After *ca.* 1 h at room temperature, solvent was removed *in vacuo* and CH_2Cl_2–light petroleum (5 cm^3, 1:1) added to the residue. This was chromatographed at −30 °C, eluting initially with the same solvent mixture to yield a yellow fraction. Removal of solvent *in vacuo* followed by crystallization from CH_2Cl_2–light petroleum (10 cm^3, 1:4) gave yellow microcrystals of $[3,3,3\text{-}(CO)_3\text{-}3,8\text{-}(Pt\{Ph_2P(CH_2)_2PPh_2\})\text{-}closo\text{-}3,1,2\text{-}ReC_2B_9H_{10}]$ **3b** (0.02 g). A second yellow fraction was eluted from the column using a 3:2 mixture of CH_2Cl_2–light petroleum. Removal of solvent *in vacuo* and crystallization from CH_2Cl_2–light petroleum (10 cm^3, 2:3) produced yellow microcrystals of $[3,3,3\text{-}(CO)_3\text{-}3,4\text{-}(Pt\{Ph_2P(CH_2)_2PPh_2\})\text{-}closo\text{-}3,1,2\text{-}ReC_2B_9H_{10}]$ **3a** (0.04 g).

$[3,3,3\text{-}(CO)_3\text{-}3,n\text{-}\{Pt(PEt_3)_2\}\text{-}closo\text{-}3,1,2\text{-}ReC_2B_9H_{10}]$ (n = 4 or 8). To the compounds $[PtCl(H)(PEt_3)_2]$ (0.17 g, 0.36 mmol) and $Ag[BF_4]$ (0.08 g, 0.41 mmol) was added THF (15 cm^3) and the mixture stirred for 2 h. The suspension was filtered through Celite onto a solution of **1** (0.20 g, 0.37 mmol) in THF (5 cm^3). This was then refluxed for 4 d. Solvent was removed *in vacuo* and CH_2Cl_2 (10 cm^3) added. The mixture was filtered through Celite followed by removal of solvent *in vacuo*. The residue was taken up in CH_2Cl_2–light petroleum (5 cm^3, 2:3). Chromatographic separation at −30 °C, eluting with CH_2Cl_2–light petroleum (2:3), afforded two yellow fractions. Removal of solvent from either followed by crystallization from CH_2Cl_2–light petroleum (10 cm^3; 1:4) gave yellow microcrystals of $[3,3,3\text{-}(CO)_3\text{-}3,8\text{-}\{Pt(PEt_3)_2\}\text{-}closo\text{-}3,1,2\text{-}ReC_2B_9H_{10}]$ **4b** (0.04 g) and $[3,3,3\text{-}(CO)_3\text{-}3,4\text{-}\{Pt(PEt_3)_2\}\text{-}closo\text{-}3,1,2\text{-}ReC_2B_9H_{10}]$ **4a** (0.02 g) in order of elution.

Reaction of compound 1 with $[Pt(H)(THF)(PEt_3)_2][BF_4]$ at room temperature. The procedure was similar to that described above for the compounds **4** ($[PtCl(H)(PEt_3)_2]$ (0.09 g, 0.19 mmol), $Ag[BF_4]$ (0.04 g, 0.21 mmol), **1** (0.10 g, 0.19 mmol)), except that the reaction was carried out in CH_2Cl_2 (20 cm^3) at 25 °C for 24 h. Column chromatography at −30 °C gave a single yellow fraction upon elution with CH_2Cl_2–light petroleum (2:3). This was composed of a mixture of compounds **4a** and **5**. The former was considerably more soluble than **5** and was readily washed away upon crystallization from CH_2Cl_2–light petroleum (8 cm^3, 1:1) giving yellow microcrystals of $[3,3,3\text{-}(CO)_3\text{-}3,8\text{-}\{Pt(H)(PEt_3)\}\text{-}8\text{-}(\mu\text{-}H)\text{-}closo\text{-}3,1,2\text{-}ReC_2B_9H_{10}]$ **5** (0.05 g). The compound **4a** (0.03 g) was isolated from the washings and crystallized from CH_2Cl_2–light petroleum (10 cm^3, 1:4).

$[3,3,3\text{-}(CO)_3\text{-}3,n\text{-}\{Pt(PMe_2Ph)_2\}\text{-}closo\text{-}3,1,2\text{-}ReC_2B_9H_{10}]$ (n = 4 or 8). A similar procedure to that described for complexes **4a** and **5** was used ($[PtCl(Me)(PMe_2Ph)_2]$ (0.15 g, 0.29 mmol), $Ag[BF_4]$ (0.06 g, 0.31 mmol), **1** (0.15 g, 0.28 mmol)), but with just 1 h stirring in CH_2Cl_2 at 25 °C. Chromatographic purification at −30 °C (CH_2Cl_2–light petroleum, 1:1) gave a single yellow fraction of $[3,3,3\text{-}(CO)_3\text{-}3,4\text{-}\{Pt(PMe_2Ph)_2\}\text{-}closo\text{-}3,1,2\text{-}ReC_2B_9H_{10}]$ **6a** (0.03 g). Stirring in CH_2Cl_2 for 24 h led to 50% isomerization to $[3,3,3\text{-}(CO)_3\text{-}3,8\text{-}\{Pt(PMe_2Ph)_2\}\text{-}closo\text{-}3,1,2\text{-}ReC_2B_9H_{10}]$ **6b**.

Crystallography

Crystals of complex **2b** were grown by evaporation from a CH_2Cl_2 solution, while those of **3a** were grown by diffusion of light petroleum into CH_2Cl_2 solutions. Both complexes co-crystallized with a molecule of CH_2Cl_2 in the asymmetric unit. A crystal of **2b** was mounted on a glass fiber and data were collected on a Siemens SMART CCD area-detector three-circle diffractometer. A full sphere of data were set to collect, but unfortunately the crystal decomposed before the data collection could be completed and the raw data were corrected accordingly. However there was still a substantial redundancy in data allowing for empirical absorption corrections (SADABS[17]) to be applied using multiple measurements of equivalent reflections. The data frames were integrated using SAINT.[17] For **3a** diffracted intensities were collected on an Enraf-Nonius CAD-4 diffractometer. No crystal decay was detected during the data collection. The data were corrected for Lorentz, polarization and X-ray absorption effects, the latter by a semi-empirical method based on azimuthal scans of ψ data of several Euclerian angles (χ) near 90°.

Both structures were solved by conventional direct methods and refined by full-matrix least squares on all F^2 data using Siemens SHELXTL version 5.03 or SHELXTL 93 and SHELXTL 97.[17] For **3a** the non-hydrogen atoms were refined with anisotropic thermal parameters. For **2b** all non-hydrogen atoms were refined anisotropically (with restrictions placed to generate sensible ellipsoids) with the exception of cage boron atoms B(3) and B(5) and the phenyl carbon atom C(106) which were refined with isotropic thermal parameters. All four phenyl rings in this structure were constrained to be planar. Cage carbon atoms were identified from the magnitudes of their anisotropic thermal parameters and from a comparison of the bond lengths to adjacent boron atoms. The agostic B–H⋯Pt hydrogen atom H(4) in complex **2b** was located ($U_{iso} = 1.5U_{iso}$[B(4)]), but its position not refined. All other hydrogen atoms were included in calculated positions and allowed to ride on the parent boron or carbon atoms with isotropic thermal parameters ($U_{iso} = 1.2U_{iso}$ of the parent atom except for the B–H hydrogen atoms in **2b** where $U_{iso} = 1.5U_{iso}$).

Table 7 Data for crystal structure analyses of complexes **2b** and **3a**

	2b	**3a**
Chemical formula	$C_{31}H_{35}B_{10}F_4O_3P_2PtRe\cdot CH_2Cl_2$	$C_{31}H_{34}B_9O_3P_2PtRe\cdot CH_2Cl_2$
M	1167.85	1080.03
T/K	292(2)	293(2)
Colour, habit	Yellow prism	Orange-yellow parallelopiped
Crystal size/mm	0.55 × 0.35 × 0.30	0.24 × 0.22 × 0.18
Crystal system	Triclinic	Triclinic
Space group	$P\bar{1}$	$P\bar{1}$
a/Å	12.122(3)	11.302(2)
b/Å	13.084(2)	13.0493(12)
c/Å	15.155(3)	15.508(4)
α/°	110.42(2)	66.198(14)
β/°	106.75(2)	80.29(2)
γ/°	92.59(2)	66.735(10)
U/Å^3	2128.5(8)	1922.4(5)
Z	2	2
μ(Mo-Kα)/mm^{-1}	6.374	7.035
No. reflections collected	8730	5329
No. independent reflections	6816	5019
R(int)	0.061	0.037
Final residuals $wR2$,[a] $R1$[b]	0.146, 0.065	0.126, 0.053
Weighting factors a, b[a]	0.0432, 0.0	0.0517, 0.5597
Largest difference peak, hole/e Å^{-3}	2.047, −1.781	1.936, −1.296

[a] Structure was refined on F_o^2 using all data: $wR2 = [\Sigma[w(F_o^2 - F_c^2)^2]/\Sigma w(F_o^2)^2]^{1/2}$ where $w^{-1} = [\sigma^2(F_o^2) + (aP)^2 + bP]$ and $P = [\max(F_o^2,0) + 2F_c^2]/3$. [b] The value is given for comparison with refinements based on F_o with a typical threshold of $F_o > 4\sigma(F_o)$ and $R1 = \Sigma||F_o| - |F_c||/\Sigma|F_o|$ and $w^{-1} = [\sigma^2(F_o) + gF_o^2]$.

Large residual peaks due to absorption effects were located close to the metal centers in both structures. All calculations were carried out on Silicon Graphics Iris, Indigo or Indy or Dell computers and the experimental data are summarized in Table 7.

CCDC reference number 186/1953.

See http://www.rsc.org/suppdata/dt/b0/b002043p/ for crystallographic files in .cif format.

Acknowledgements

We thank the Robert A. Welch Foundation for support (Grant AA-1201), and Dr John C. Jeffery (Bristol University) for assistance in acquiring the crystallographic data for complex **2b**.

References

1 R. J. Puddephatt and J. Xiao, *Coord. Chem. Rev.*, 1995, **143**, 457 and refs. cited therein; M. Bergamo, T. Beringhelli, G. Ciani, G. D'Alfonso, M. Moret and A. Sironi, *Organometallics*, 1996, **15**, 1637 and refs. cited therein; C. P. Casey, E. W. Rutter Jr. and K. J. Haller, *J. Am. Chem. Soc.*, 1987, **109**, 6886; S. W. Carr, X. L. R. Fontaine, B. L. Shaw and M. Thornton-Pett, *J. Chem. Soc.*, *Dalton Trans.*, 1988, 769.

2 I. Blandford, J. C. Jeffery, P. A. Jelliss and F. G. A. Stone, *Organometallics*, 1998, **17**, 1402.

3 M. F. Hawthorne and T. D. Andrews, *J. Am. Chem. Soc.*, 1965, **87**, 2496; T. D. Andrews, M. F. Hawthorne, D. V. Howe, R. L. Pilling, D. Pitts, M. Reintjes, L. F. Warren Jr., P. A. Wegner and D. C. Young, *J. Am. Chem. Soc.*, 1968, **90**, 879.

4 D. D. Ellis, P. A. Jelliss and F. G. A. Stone, *Organometallics*, 1999, **18**, 4982.

5 M. J. Attfield, J. A. K. Howard, A. N. de M. Jelfs, C. M. Nunn and F. G. A. Stone, *J. Chem. Soc.*, *Dalton Trans.*, 1987, 2219.

6 H. C. Kang, S. S. Lee, C. B. Knobler and M. F. Hawthorne, *Inorg. Chem.*, 1991, **30**, 2024; N. L. Douek and A. J. Welch, *J. Chem. Soc.*, *Dalton Trans.*, 1993, 1917; Y.-K. Yan and M. P. Mingos, *Chem. Soc. Rev.*, 1995, 203; G. Ferguson, J. Pollock, P. A. McEneany, D. P. O'Connell, T. R. Spalding, J. F. Gallagher, R. Macias and J. D. Kennedy, *Chem. Commun.*, 1996, 679.

7 (*a*) D. D. Devore, J. A. K. Howard, J. C. Jeffery, M. U. Pilotti and F. G. A. Stone, *J. Chem. Soc.*, *Dalton Trans.*, 1989, 303; (*b*) J. E. Goldberg, D. F. Mullica, E. L. Sappenfield and F. G. A. Stone, *J. Chem. Soc.*, *Dalton Trans.*, 1992, 2693; (*c*) S. J. Dossett, D. F. Mullica, E. L. Sappenfield, F. G. A. Stone and M. J. Went, *J. Chem. Soc.*, *Dalton Trans.*, 1993, 281; (*d*) J. E. Goldberg, J. A. K. Howard, H. Müller, M. U. Pilotti and F. G. A. Stone, *J. Chem. Soc.*, *Dalton Trans.*, 1990, 3055; (*e*) J. C. Jeffery, P. A. Jelliss and F. G. A. Stone, *Inorg. Chem.*, 1993, **32**, 3943.

8 (*a*) N. Carr, M. C. Gimeno and F. G. A. Stone, *J. Chem. Soc.*, *Dalton Trans.*, 1990, 2617; (*b*) S. Anderson, D. F. Mullica, E. L. Sappenfield and F. G. A. Stone, *Organometallics*, 1995, **14**, 3516.

9 R. J. Blau and J. H. Espenson, *Inorg. Chem.*, 1986, **25**, 878.

10 J. C. Jeffery, M. A. Ruiz, P. Sherwood and F. G. A. Stone, *J. Chem. Soc.*, *Dalton Trans.*, 1989, 1845; S. L. Hendershot, J. C. Jeffery, P. A. Jelliss, D. F. Mullica, E. L. Sappenfield and F. G. A. Stone, *Inorg. Chem.*, 1996, **35**, 6561.

11 D. M. Roundhill, *Adv. Organomet. Chem.*, 1975, **13**, 273; H. D. Kaesz and R. B. Saillant, *Chem. Rev.*, 1972, **72**, 231.

12 F. G. A. Stone, *Adv. Organomet. Chem.*, 1990, **31**, 53; S. A. Brew and F. G. A. Stone, *Adv. Organomet. Chem.*, 1993, **35**, 135; P. A. Jelliss and F. G. A. Stone, *J. Organomet. Chem.*, 1995, **500**, 307.

13 J. A. Long, T. B. Marder, P. E. Behnken and M. F. Hawthorne, *J. Am. Chem. Soc.*, 1984, **106**, 2979; I. T. Chizhevsky, I. A. Lobanova, V. I. Bregadze, P. V. Petrovskii, V. A. Antonovich, A. V. Polyakov, A. I. Yanovskii and Y. T. Struchkov, *Mendeleev Commun.*, 1991, 48; J. C. Jeffery, P. A. Jelliss and F. G. A. Stone, *J. Chem. Soc.*, *Dalton Trans.*, 1993, 1073; A. Franken, J. Kautz, F. G. A. Stone and P.-Y. Yu, *Organometallics*, 2000, **20**, 1993.

14 F. R. Hartley, in *Comprehensive Organometallic Chemistry*, eds. E. W. Abel, F. G. A. Stone, G. Wilkinson, Pergamon (Elsevier Science Ltd), Oxford, 1982, vol. 6, sect. 39.5.1.5(i).

15 G. W. Parshall, *Inorg. Synth.*, 1970, **12**, 28.

16 G. K. Anderson and M. Lin, *Inorg. Synth.*, 1990, **28**, 60.

17 Siemens X-Ray Instruments, Madison, WI, 1995.